Ordering kinetics in the long-period superlattice alloy $Cu_{0.79}Pd_{0.21}$

X. Wang, J. Mainville, and K. Ludwig
Department of Physics, Boston University, Boston, Massachusetts 02215, USA

X. Flament and A. Finel
ONERA-LEM, Boîte Postale 72-29 avenue de la division Leclerc, 92322 Châtillon, France

R. Caudron
ONERA-LEM, Boîte Postale 72-29 avenue de la division Leclerc, 92322 Châtillon, France and Laboratoire Léon Brillouin (CEA-CNRS), CEA Saclay, 91191 Gif-sur-Yvette, France

(Received 30 August 2004; revised manuscript received 25 April 2005; published 28 July 2005)

The kinetics of long-period superlattice (LPS) formation from the disordered state has been examined in a $Cu_{0.79}Pd_{0.21}$ alloy that exhibits a one-dimensional LPS ordered state. Time-resolved x-ray scattering shows that, following a rapid temperature quench from the disordered state into the LPS region of the phase diagram, the satellite peaks initially grow more quickly than do the central integer-order superlattice peaks. During this process, the satellite peak position, which is inversely related to the average modulation wavelength $2M$, initially decreases rapidly, then reaches a minimum and relaxes slowly back toward its new equilibrium position. In the later stages of the LPS formation process, the satellite and central integer-order superlattice peaks narrow in a manner consistent with $t^{1/2}$ domain coarsening. A simple stochastic model of the partially ordered structure was developed to better understand the relationships between peak widths.

DOI: 10.1103/PhysRevB.72.024215 PACS number(s): 61.10.Eq, 64.60.Cn, 83.10.Tv

I. INTRODUCTION

The kinetics of phase transformations in alloys continues to be an important topic from both fundamental and technological viewpoints. In developing a basic understanding of alloy phases and kinetics, long-period superlattice (LPS) alloys present particularly intriguing challenges. These systems are characterized by the existence of an ordered phase in which there is a modulation of the local order between antiphase domains. The formation kinetics of such complex structures from the disordered state has been little investigated. Here we describe a detailed study of the ordering kinetics in a classic LPS system, Cu-Pd, in the composition range where the equilibrium ordered state of interest has a one-dimensional modulated structure.[1–5] The kinetics was investigated experimentally using synchrotron-based time-resolved x-ray diffraction. In addition, a simple stochastic model of the partially ordered structure was developed to understand the relative peak widths in different reciprocal space directions.

II. Cu-Pd ALLOY STRUCTURE

The Cu-rich Cu-Pd alloys exhibit structures based upon face-centered-cubic (fcc) lattices. In the high-temperature disordered structure, Cu and Pd atoms occupy fcc sites at random, though short-range chemical order (SRO) exists. In the $L1_2$ ordered structure with ideal stoichiometry Cu_3Pd, Cu atoms preferentially occupy face centers and Pd atoms preferentially occupy corners of the unit cell. Since there are four equivalent sites in the fcc unit cell, there is a factor of 4 degeneracy in the $L1_2$ ordered structure. Antiphase boundaries (APB's) between ordered regions can be either "conservative" or "nonconservative."[6] A conservative APB separates two ordered regions that differ from each other by a translation vector parallel to the plane of the APB interface. In this case, the local stoichiometry at the interface remains unchanged. A nonconservative APB separates two ordered regions that differ from each by a translation vector with a component perpendicular to the APB interface. In this case the local stoichiometry of the interface is changed. In the $L1_2$ structure region of a phase diagram, there is a free-energy cost to forming APB's, and none exist in equilibrium. Because the nearest-neighbor atomic environment is not changed by the presence of conservative APB's, these are typically lower in energy than nonconservative APB's.

In contrast to the situation for the $L1_2$ structure, LPS alloy phases contain APB's as an integral part of their structure. Thus they exhibit a modulation of the order, with average domain size M between APB's. The Cu-Pd alloys are a classic LPS system with one-dimensional (1D) modulated structures at Pd concentrations of approximately 18%–28% and two-dimensional (2D) modulated structures at elevated temperatures and Pd concentrations of approximately 24%–32%.[7] The APB's in the 1D LPS state are conservative, while in the 2D LPS state, one direction has conservative APB's while the other direction has nonconservative APB's. Below approximately 23% Pd, the 1D LPS states are incommensurate and have a period ($5 \leqslant M \leqslant 15$) which varies continuously with concentration and temperature. At higher Pd compositions, the 1D LPS states are commensurate ($3 \leqslant M \leqslant 5$) and do not change much with temperature.

Much of the equilibrium behavior of the Cu-Pd system has been explained using Fermi surface arguments.[8–11] Using KKR-CPA electronic calculations, Ceder *et al.*[12] have calculated effective pair interactions which, when put into a mean-

field model, qualitatively reproduce the 1D LPS states found in Cu-Pd alloys. The presence of antiphase correlations in the disordered state has also been associated with Fermi surface nesting in the ⟨110⟩ directions. This is believed to lead to Friedel-type oscillations in the effective pair interaction between atoms in this direction. Analogies have also been drawn between LPS alloy behavior and that of the axial next-nearest-neighbor Ising (ANNNI) model.[13] In the ANNNI model, modulated phases are stabilized by entropic rather than enthalpic effects.

The diffraction pattern from a $L1_2$ structure exhibits "fundamental" Bragg peaks for which the crystallographic indices $(h\,k\,l)$ are all of the same parity. These are independent of the degree of order, and thus exist even in the fcc disordered state. The $L1_2$ ordering, i.e., the alternation of pure and mixed planes, also produces peaks at the integer-order "superlattice" reciprocal lattice points where h, k, and l are not all of the same parity. If the ordering is imperfect, then the superlattice peaks are broadened. However, because conservative APB's separate regions of order that differ by a vector that lies in the plane of the interface, their presence causes an anisotropic broadening of the integer-order superlattice peaks. Thus integer-order superlattice peaks typically exhibit a "pancake" shape in reciprocal space, with the short dimension of the pancake being inversely proportional to the average distance between nonconservative APB's, and the long pancake dimension inversely proportional to the average distance between a combination of conservative and nonconservative APB's.[6]

In addition to the $L1_2$ integer-order superlattice peaks at appropriate integral reciprocal lattice positions, the reciprocal space structure of the 1D LPS phase of Cu-Pd alloys has satellite peaks separated from these by $q_0=(2M)^{-1}$. Figure 1(a) shows the scattering for a single variant of the ordered alloy with the long-period modulation along the [001] direction. For a Cu-Pd sample consisting of all three possible variants, there are four satellites in a plane around each central integer-order superlattice point, as shown in Fig. 1(b). Finally, in the disordered state, above the order-disorder transition, antiphase fluctuations still give rise to diffuse satellite peaks, but the peaks at the reciprocal space positions disappear, as diagramed in Fig. 1(c).

For simplicity, we will refer to the [001] direction normal to the plane of the four satellites as "out-of-plane." Note that an "out-of-plane" scan defined in this fashion need not necessarily pass through the (001) reciprocal space point. Thus a scan from the (0 0 0.9) through the (0 0 1) reciprocal lattice points is "out-of-plane," but so is one from the $(0\ q_0\ 0.9)$ through the $(0\ q_0\ 1.0)$ by this definition.

Experimentally, we typically find little difference in peak widths in different directions within the plane of the satellites. We will simply refer to *all* directions in the plane of the satellites as "in-plane." Thus a scan passing from the (0 0 1) through the $(0\ q_0\ 1)$ reciprocal lattice points would be an "in-plane" scan, as would one passing from the (0 0 1) through the $(q_0\ 0\ 1)$.

III. EXPERIMENTAL DETAILS

Experiments were performed on a polished (0 0 1) cut $Cu_{0.79}Pd_{0.21}$ single crystal grown at the Office National d'Etudes et de Recherches Aérospatiales (ONERA). The composition was verified by microprobe. The x-ray rocking curve width of the crystal, giving the mosaic spread, was 0.2 ° HWHM. At the temperatures studied, these crystals typically exhibited equilibrium antiphase domain sizes in the ordered state of $M \approx 5.8-6$. During the real-time x-ray experiments, the sample was heated inside a small high vacuum chamber with a hemispherical beryllium window to allow optimal x-ray access. The furnace utilized a boron-nitride heater heat sunk to a water-cooled copper block. To promote temperature uniformity during the kinetics experiments, helium gas was flowed through the chamber with 1 atm pressure during experiments. The helium was initially rated 99.999% pure. Before entering the chamber, it passed through a Ti gettering furnace to remove any residual oxygen and water vapor. An oxygen sensor monitored the exhaust gas flow; it routinely measured less than 10^{-6} ppm oxygen contamination. After over 20 hours of experimentation at high temperature, no oxidation of the crystal was visible by eye. A thermocouple mounted in the sample holder directly beneath the crystal measured the sample temperature. Over-

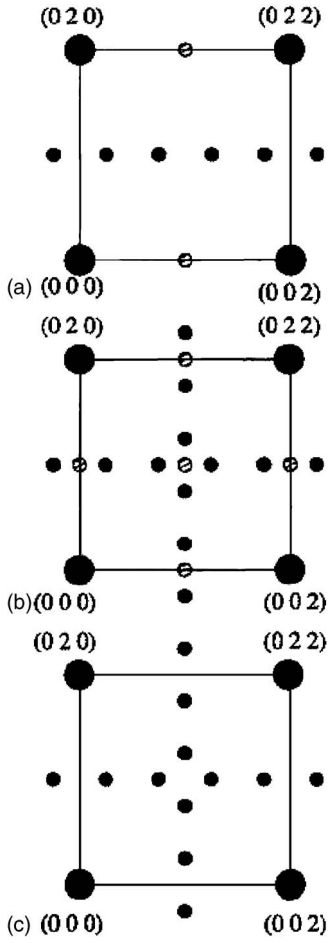

FIG. 1. Comparison of the diffraction patterns from the 1D LPS phase and the disordered phase of Cu-Pd. Large solid circles denote fundamental peaks; small hatched circles denote superlattice peaks; small solid circles denote satellite peaks. (a) A single variant with the long-period modulation along the [0 0 1] direction; (b) all three variants present; (c) center of diffuse peaks in the disordered phase.

all this thermal geometry typically allowed the crystal to be rapidly cooled by $\Delta T \sim 100$ K and thermally stabilized in 8 s. Absolute temperatures were calibrated with thin-film alloys of Si-Au, Si-Ag, and Si-Al, which have published eutectic temperature of 636 K, 850 K, and 1108 K (Ref. 14), respectively.

Kinetics experiments were performed on beam line X20C of the National Synchrotron Light Source (NSLS) at Brookhaven National Laboratory. Experiments used either a high-flux wide-bandpass W-Si multilayer monochromator ($\delta E/E \approx 1.5\%$) or a high-resolution Si(111) monochromator. In both cases the photon energy was 6.90 keV and typical beam size was 0.4 mm $\times$ 0.4 mm. The scattering was measured with a CCD-based x-ray area detector from Princeton Instruments Corporation. Typical time resolution was approximately 1 s. Because the x-ray angle of incidence was fixed at $\theta \approx 15° - 20°$ in the experiments, the area detector monitored the structure factor evolution over a slightly curved surface in reciprocal space that was inclined by an angle θ with respect to the out-of-plane direction. For late-stage kinetics studies in which domain sizes became large, the observed peak line shapes were corrected by removing the experimental resolution function. Using the high-resolution Si monochromator, typical instrumental resolution broadening in the reciprocal space region of interest (including crystal mosaic spread) was approximately 0.002 reciprocal lattice units (rlu) in the out-of-plane direction and 0.004 rlu in the in-plane direction. The accuracy of these numbers was verified in a scan of the fundamental (0 0 2) Bragg peak. In addition to the kinetics data presented here, we have earlier published a diffuse x-ray scattering study of the disordered state of this crystal.[15]

IV. EXPERIMENTAL RESULTS

A. Equilibrium behavior

We have previously reported the equilibrium behavior of the short-range order fluctuations in the high temperature disordered state in this sample.[15] The transition temperature between the disordered and LPS phases was estimated using slow (2 K/min) ramps up in temperature while monitoring the intensity of the satellite peaks in a state that was initially well ordered. Figure 2 shows such a ramp scan, with an estimated transition temperature of approximately 765 K. Extrapolations of the diffuse scattering intensity above the transition suggest the presence of an ordering spinodal at approximately 751 K, so that the ordering spinodal is depressed below the first-order transition by less than 2%. Published phase diagrams[7] suggest that the two-phase region near the transition is small—only a few degrees in width.

Using a Ginzburg–Landau free-energy, Finel[16] has shown that the low-order coupling between satellite and integer-order superlattice ordering waves leads to a difference in their equilibrium temperature dependence below the transition.[17] In particular, this model suggests that there is a primary order parameter associated with the satellite peaks which should increase with temperature below an effective critical point T_c as $(T_c - T)^{1/2}$. The model predicts that a secondary order parameter associated with the integer-order superlattice peaks should increase as $(T_c - T)$. In a kinematic scattering approximation, the intensity of the x-ray Bragg peaks should be proportional to the square of the order parameter if ordered domain sizes are constant. Thus this model would predict that the satellite peaks should exhibit a $(T_c - T)$ temperature dependence while the central integer-order superlattice peaks should exhibit a $(T_c - T)^2$ temperature dependence. Although we have not examined this prediction in detail, we note that the data of Fig. 2 is qualitatively in accord with Finel's prediction. The satellite peak intensity starts growing before the integer-order superlattice peak intensity with decreasing temperature below the transition.

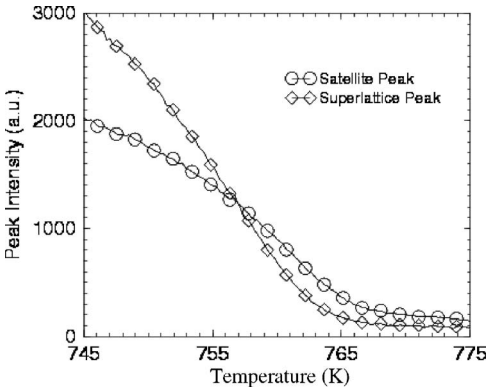

FIG. 2. Variation of superlattice and satellite intensities as a function of temperature. Data was taken with a ramp rate upward of 2 K/min. A phase transition temperature of 765 K is estimated from the change in curvature of the peak intensities.

B. Initial ordering kinetics

In our studies of the ordering kinetics, the crystal was typically equilibrated at 803 K in the disordered state before quenching to a temperature below the phase transition to follow the kinetic evolution. The scattering was examined in the vicinity of both (0 0 1) and (0 1 1) superlattice points, as well as the (0 0 2) fundamental peak. Using the area detector, two of the four satellites could be simultaneously observed near the (0 0 1). All four satellites could be observed simultaneously near the (0 1 1), though they could not all four be brought into the ideal diffraction condition for the area detector simultaneously. Two CCD frames from a typical ordering process are shown in Fig. 3. The various peaks are sensitive to different LPS ordered variants. An ordered variant with the antiphase modulation perpendicular to the sample surface (i.e., along the [0 0 1] direction) gives rise to a peak at the (0 0 1) reciprocal lattice position and satellites at $(0\ 1\ 1 \pm q_0)$. The ordered variant in the [1 0 0] direction, i.e., in the sample plane, gives rise to a peak at the (0 1 1) superlattice position and satellites at $(\pm q_0\ 0\ 1)$. By comparing the kinetics as observed in the two different reciprocal space regions, we were able to examine to what extent the variant normal to the sample surface behaved differently than the two in-plane variants. No significant differences were observed. Moreover, we focus here on regimes in which the ordering process appears to be happening homogeneously on a fine scale much smaller than the absorption length of the x

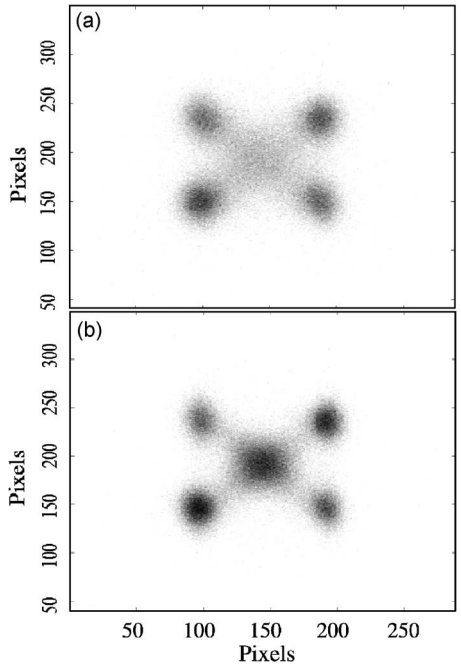

FIG. 3. Raw CCD image of the data near the (1 1 0) point during the ordering process. The central peak is the (1 1 0) and there are four neighboring satellites due to the developing antiphase correlations. (a) 980 s after quench, (b) 2980 s after quench.

rays into the crystal (several microns). Thus the kinetics results we present below are believed to be characteristic of the bulk as a whole and not influenced by the presence of the surface.

The typical quench time of 8 s allowed the sample to be quenched and equilibrated at temperature below the transition with very little change in scattering (see Fig. 4). Thus we observed isothermal kinetics from a very early stage. Observations of the (2 0 0) peak (Fig. 5) showed that the lattice relaxed during the temperature quench itself. For a quench from 803 K to 726 K, the 2θ of the peak (2 0 0) changed from 57.76 ° to 57.82°. Correspondingly, the lattice constant contracted from 0.3714 nm to 0.3710 nm, i.e., approximately

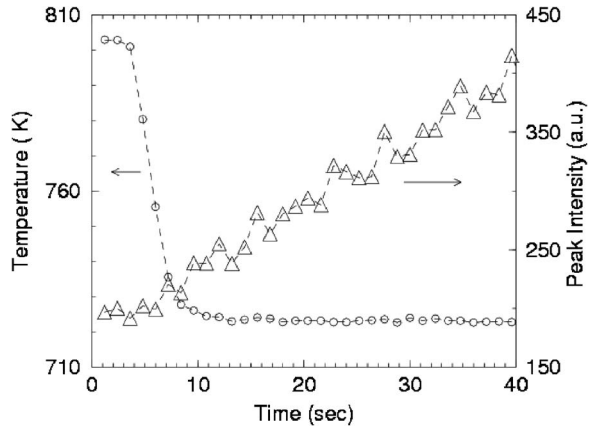

FIG. 4. The time evolution of the satellite peak intensity during and after a quenching process from 806 K to 726 K. There is very little evolution of the scattering during the quench itself.

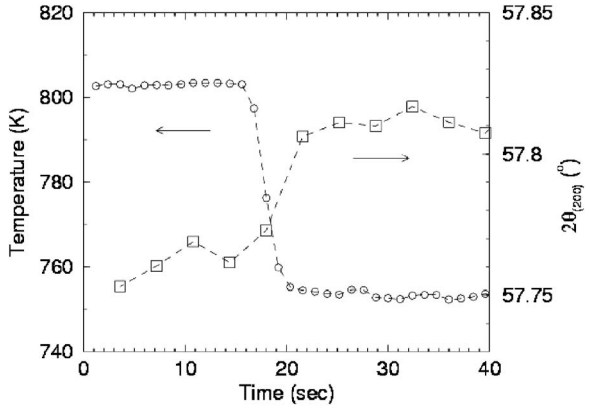

FIG. 5. The time evolution of the fundamental (2 0 0) peak during and after a quench from 803 K to 751 K.

0.09%. The linear thermal expansion coefficients for Cu and Pd are 1.7×10^{-5} K and 1.2×10^{-5} K, respectively. By assuming that the thermal expansion of the binary alloy is the molar weight average of each species, we can estimate the thermal expansion coefficient of $Cu_{0.79}Pd_{0.21}$ to be approximately 1.6×10^{-5} K. The 50 K temperature drop is thus estimated to have caused approximately 0.1% contraction. This indicates the peak shift during the quench is mostly due to thermal effect. There was no indication from the (2 0 0) peak of further lattice relaxation during the ordering process, nor did we see evidence of peak splitting associated with the small tetragonal distortion occurring in the ordered phase.

Our previous studies of the diffuse scattering in this Cu-Pd alloy[15] suggested the presence of an ordering pseudospinodal at approximately 751 K. We have examined the ordering kinetics primarily for quenches near and below this temperature. Following a rapid quench of the disordered sample into the continuous ordering regime, the satellite peaks present in the disordered phase grow and narrow much more quickly than do the peaks at the integer-order superlattice positions. This can be seen in the intensity plot of Fig. 6. Indeed, in the disordered phase and in the early stages of ordering, there is no peak at the integer-order superlattice position. Given the above considerations, this indicates that antiphase structures are forming but that the translations relating neighboring domains in the growing structures are relatively random.

The free-energy of Finel's approach[16] can be used in a Langevin equation to predict the ordering kinetics. If higher order terms are neglected, a simple linear theory[18] of continuous ordering in the alloy is obtained which suggests that, as observed, the satellite peak intensity should grow more rapidly than the integer-order superlattice intensity during the early stage of the ordering process. However, this simple linear theory also predicts exponential growth of the satellite intensity during the early stage ordering below the pseudospinodal. This is not observed; instead the satellite peak intensities always display a negative curvature (i.e., downward curvature) as a function of time. It should be pointed out that any exponential growth regime present should be easily seen, as the scattering intensity typically grows by less than 30% during the quench process itself. Such nonlinear behavior is frequently observed in metals.

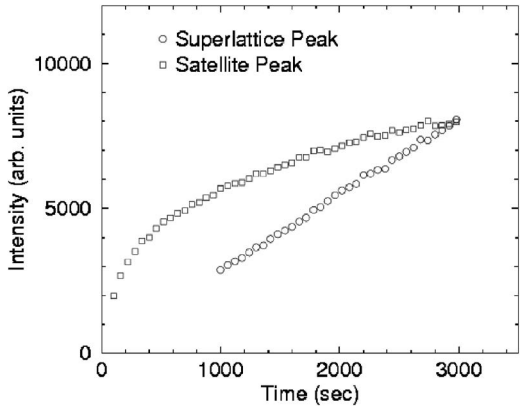

FIG. 6. The growth of peak intensities for the satellite and superlattice peak following a quench to 723 K. The zero of time is set to be when the sample temperature reaches equilibrium. Due to the complicated peak shapes arising during the kinetics, the data could not be fit at the earliest times following the quench. Only the satellite peaks appear then as distinct peaks.

The evolution of the peak widths is complex. In the satellites, the out-of-plane peak width is always slightly larger than the in-plane peak width. The central integer-order superlattice peak is very wide in the initial stages of the ordering process. As the LPS formation progresses, however, the central peak width in the out-of-plane direction becomes comparable to those of the satellites. The central peak is always significantly wider in the in-plane direction than in the out-of-plane direction.

During the very initial stages of the ordering process following a quench, the satellite peak splitting decreases, i.e., the modulation wave number q_0 decreases, suggesting that the average modulation wavelength is increasing (see Fig. 7). This follows the trend with decreasing temperature observed for the disordered alloy.[15] However, after this initial period, q_0 begins to increase again, though at a much slower rate. This effect is more pronounced at lower quench temperatures. A possible explanation for the observed nonmonotonic

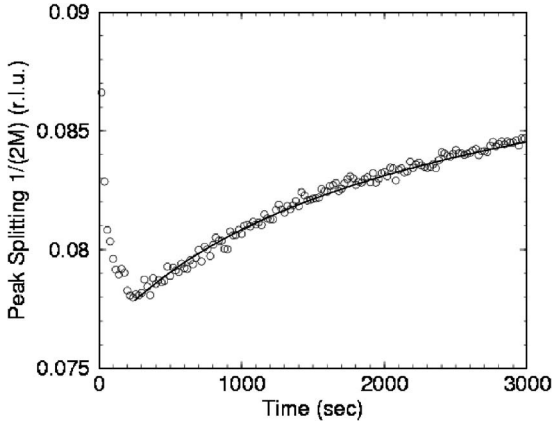

FIG. 7. The nonmonotonic change of the satellite peak splitting q_0 as a function of time following a quench to 723 K. The time for temperature equilibration is approximately 8 s. The zero of time is set to be when the sample temperature reaches equilibrium. The solid line is a fit to a power law relaxation as discussed in the text.

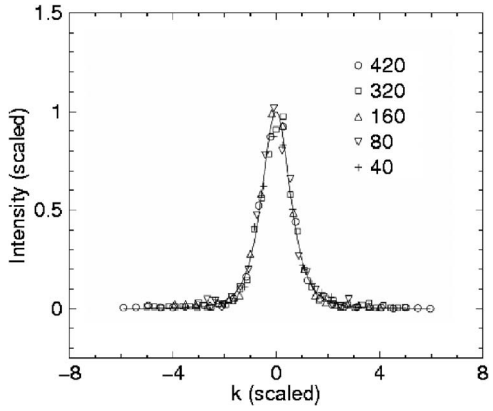

FIG. 8. The scaling behavior of the superlattice peak evolution in the out-of-plane direction. Data times after quench to 723 K shown in minutes. The solid line is the approximate scaling Lorentzian squared function.

evolution of the peak splitting is discussed in the conclusions below.

C. Late-stage kinetics

In order to investigate the late stages of the LPS ordering process, the isothermal transformation kinetics was investigated over time scales as long as 12 hours. The practical time limitations of performing experiments at the synchrotron prevented lengthier studies. At late times, the out-of-plane width of the integer-order superlattice peak becomes comparable to the out-of-plane width of the satellite peaks, but the in-plane width of the satellite peaks remains somewhat smaller than both. In contrast, the in-plane width of the integer-order superlattice peaks remained considerably larger.

In an alloy exhibiting simple ordering kinetics, the integer-order superlattice peak line shape usually exhibits a dynamic scaling during the coarsening process such that the integrated peak intensity is constant.[19] In the more complicated LPS case examined here, the anisotropic line shapes make experimental determination of the integrated intensity difficult. However, we have systematically examined the dynamic scaling of the satellite and integer-order superlattice peaks by normalizing their line shapes by their widths and peak intensity. Typical results for the (1 0 0) superlattice peak evolution in the out-of-plane direction are shown in Fig. 8. As can be seen in the figure, after approximately 40 minutes in the case of a 723 K quench, they exhibit good scaling behavior. The predicted scaling forms[19] for simple "Model A" (nonconserved order parameter)[20] coarsening kinetics can be approximated by a Lorentzian squared function which fits the data well. Similar behavior is seen in the integer-order superlattice in-plane line shape and in the satellite line shapes in both the in-plane and out-of-plane directions.

For alloys exhibiting coarsening kinetics with a nonconserved order parameter, the peak width w typically follows the Cahn-Allen law:[21] $w^{-2}-w_0^{-2}=at$, where w_0 and a are constants and t is time. In order to investigate whether the observed line-shape evolution is consistent with the Cahn-Allen

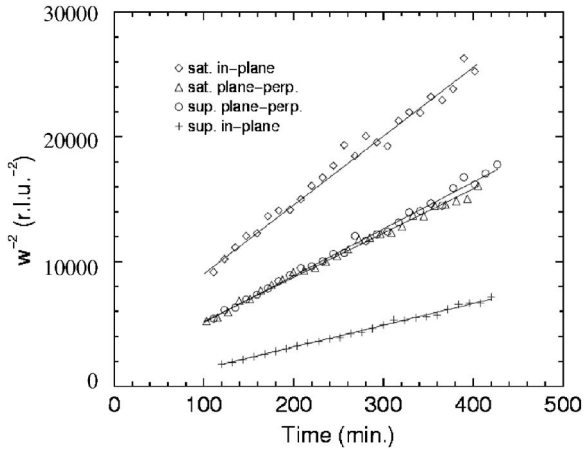

FIG. 9. Inverse peak width squared as a function of time for integer-order superlattice ("sup") and satellite ("sat") peaks in the in-plane and out-of-plane ("plane-perp") directions after a quench to 723 K.

law, we have plotted w^2 as a function of time; Fig. 9 shows the result for different peak widths for a quench to 723 K. Reasonably good linear behavior is observed for all four.

The slope of the Cahn-Allen curves increases systematically with increasing quench temperature, as shown in Fig. 10. This is expected since the constant a in the Cahn-Allen law is proportional to the atomic diffusivity, which itself should be thermally activated. In Fig. 11, an Arrhenius semilog plot of the experimental a values does show an approximately straight line, with a slope corresponding to an activation energy of 2.7 ± 0.3 eV. Although we cannot find any measured values of the diffusion activation energy in Cu-Pd alloys near this composition, this value is somewhat larger than the published activation energy (1.66 ± 0.23 eV) for interdiffusion in Cu/Pd multilayers.[22] While we are not in a position to independently measure the vacancy equilibration time following a quench in the crystal studied, the high activation energy measured here suggests that the vacancy concentration has equilibrated by the onset of late-stage coarsening.

We conclude, then, that the late-stage kinetics appears to be consistent with the Cahn-Allen prediction, despite the

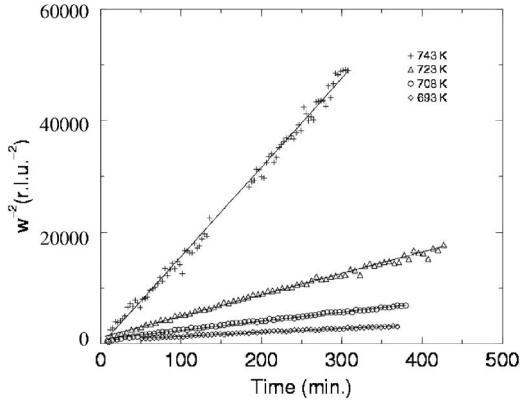

FIG. 10. Inverse peak width squared as a function of time for the superlattice peak in the radial direction at different quench temperatures.

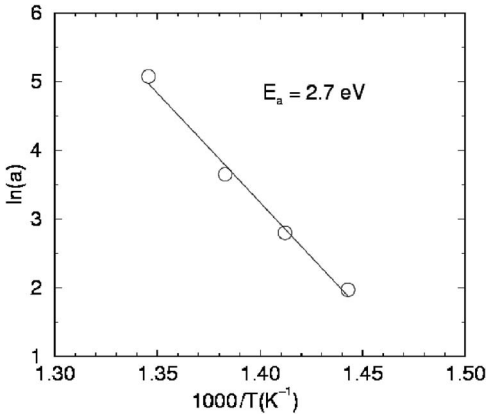

FIG. 11. Arrhenius plot of the prefactor a in the Cahn-Allen law.

complexities of the LPS structure. It is noteworthy that theoretical investigations of coarsening in ANNNI models have also found agreement with the Cahn-Allen $w\sim t^{1/2}$ prediction.[23,24]

V. STOCHASTIC MODEL OF OBSERVED RECIPROCAL SPACE STRUCTURE

It would be interesting to undertake a detailed microscopic modeling at the atomic scale to reproduce the correct statistical fluctuations that lead to the APB dynamics, and to the related peak profiles. This has not been done here. However, some insight into the causes of the observed relative peak widths and intensities (integer-order superlattice and satellite) can be gained from a simple stochastic model of the partially ordered structure with periodic APB's following the method of Hendricks and Teller.[25] This model only treats the statistics of consecutive APB's, with a fixed spacing between them. All smaller scale fluctuations are ignored. Despite its simplifying assumptions, this model reproduces the main characteristics of the experimental observations.

Consider, for simplicity, a square-wave antiphase modulation in the x direction with six unit cells of one ordered sublattice followed by six unit cells of a different ordered sublattice, forming a modulated structure with short-range order. As mentioned above, there are four possible sublattices on which atoms can order in the $L1_2$ structure. Given an antiphase domain ordered on one sublattice, there are three possibilities for the next antiphase domain in the sequence. One of those three possibilities will have a conservative APB with the original antiphase domain. Thus, this boundary will have a low energy, and we denote the probability that this particular sublattice follows the original as $\gamma_x \leqslant 1$. Alternatively, one of the other possible ordered sublattices (which have higher energy nonconservative APB's with respect to the first domain) could follow the original with a probability $\eta_x=\frac{1}{2}(1-\gamma_x)$. In the two directions perpendicular to the modulation (i.e., the y and z directions), at each unit cell there is the possibility of a change of sublattice ordering (i.e., a nonequilibrium domain wall). We take the probability that there is a conservative domain wall between two unit cell

neighbors in the y or z directions to be γ_y. The probability that there is a nonconservative domain wall between two unit cell neighbors in the y or z directions is taken as $2\eta_y$. The probability that no APB occurs between given neighboring unit cells in the y and z directions is then $(1-\gamma_y-2\eta_y)$. For simplicity we assume no correlations between APB's in the x, y, and z directions. Then the scattered intensity can be written as

$$I(h,k,l) = \Gamma_{x1}\Gamma_{y1}\Gamma_{z2}|F_1+F_2-F_3-F_4|^2 + \Gamma_{x1}\Gamma_{y2}\Gamma_{z1}|F_1-F_2 + F_3-F_4|^2 + \Gamma_{x2}\Gamma_{y1}\Gamma_{z1}|F_1-F_2-F_3+F_4|^2, \quad (1)$$

where

$$\Gamma_{x1} = \frac{1-\gamma_x^2}{1+\gamma_x^2+2\gamma_x\cos(12\pi h)}, \quad (2)$$

$$\Gamma_{x2} = \frac{2\gamma_x(1-\gamma_x)}{1-2\gamma_x(1-\gamma_x)-(2\gamma_x-1)\cos(12\pi h)}, \quad (3)$$

$$\Gamma_{y1} = \frac{1-(1-2\gamma_y-2\eta_y)^2}{1+(1-2\gamma_y-2\eta_y)^2-2(1-2\gamma_y-2\eta_y)\cos(2\pi k)}, \quad (4)$$

and

$$\Gamma_{y2} = \frac{1-(1-4\eta_y)^2}{1+(1-4\eta_y)^2-2(1-4\eta_y)\cos(2\pi k)}. \quad (5)$$

The Γ_{z1} and Γ_{z2} are similar to the Γ_{y1} and Γ_{y2} but with the reciprocal space coordinate "k" replaced by "l." The F_1, F_2, F_3, and F_4 are the structure factors for "super" unit cells six fcc unit cells long in the x direction. They are ordered on the four possible sublattices, in particular with the Pd site at (0 0 0), (1 1 0), (1 0 1) and (0 1 1), respectively.

A key attribute of this simple model is that it correctly incorporates the phase relationships across APB's. In the limit that the lattice is becoming well ordered with $(1-\gamma_x) \ll 1$ and $\gamma_y, \eta_y \ll 1$, the Γ terms reduce to Lorentzian line shapes near the appropriate satellite and integer-order superlattice peaks. The HWHM of a satellite peak in the x direction (which is a "in-plane" direction in our previous terminology) is $(12\pi)^{-1}(1-\gamma_x)=(6\pi)^{-1}\eta_x$. The HWHM of an integer-order superlattice peak for the modulated structure [e.g., (1 0 0)] in the out-of-plane direction is $(6\pi)^{-1}(1-\gamma_x) = (3\pi)^{-1}\eta_x$. Thus, we see that broadening of the satellite and integer-order superlattice peaks in these directions is simply proportional to the probability of encountering a nonconservative APB. However, because of the phase relationships across the relevant APB's, the model predicts that the width of the integer-order superlattice peaks in the out-of-plane direction is twice the width of the satellite peaks in the in-plane modulation direction (the x direction in this case). The data of Fig. 9 are consistent with the direction of this effect, though the actual peak width ratio is somewhat less than a factor of 2.

In this same well-ordered limit, the in-plane width of an integer-order superlattice peak of the modulated structure is $\pi^{-1}(\gamma_y+\eta_y)$. Two terms contribute to the out-of-plane width of a satellite peak. If we assume that conservative APB's are much more common than nonconservative APB's (i.e. $\gamma_y \gg \eta_y$), then the satellite out-of-plane peak width becomes $(2/\pi)\eta_y$. In this limit, this is much smaller than the in-plane integer-order superlattice peak width of $\pi^{-1}(\gamma_y+\eta_y)$. Indeed, the data of Fig. 9 are consistent with a ratio of γ_y to η_y of 3–4.

A final striking feature of Fig. 9 is that the out-of-plane peak widths of the integer-order superlattice and satellite peaks are essentially equal. This is easily understood from this model if $\eta_x=6\eta_y$. Since η_x is defined as the probability of having a nonconservative APB every six unit cells, while η_y is defined as the probability of having a nonconservative APB between neighboring unit cells, this result simply means that nonconservative APB's are equally likely in the modulated direction and in the two perpendicular directions.

Thus this simple stochastic model, despite its limitations, explains the main features of our experiments.

VI. DISCUSSION AND CONCLUSIONS

As seen in the experimental kinetics data, the processes by which Cu-Pd alloys develop a one-dimensional LPS structure from the disordered state are complex. However, though we are not yet in a position of being able to understand the observed behavior quantitatively, much of the kinetics behavior can perhaps be understood at a qualitative level.

The detailed time-resolved x-ray scattering data show that during the ordering process, concentration waves at the satellite positions initially grow more rapidly than do those at the integer-order superlattice positions. As discussed above, this is consistent with a Ginzburg-Landau free-energy functional approach in which the ordering instability is associated with the modulation wave vectors. This approach also correctly predicts the observed relative equilibrium behavior of the modulated and integer-order superlattice order parameters just below the transition point.

A second qualitative observation is the nonmonotonic evolution of the average modulation wave number q_0. As noted above, the initial decrease of q_0 following a quench is consistent with the direction of the equilibrium change in splitting with temperature above the transition.[15] It is possible that the subsequent slow increase in q_0 may be associated with defects at the boundaries between local regions of LPS order.[26] If so, we would expect the effect of such interfacial defects to decrease as the density of interfaces increases, i.e., as the average domain size grows. As discussed above, the Cahn-Allen growth appears to be applicable during the coarsening of domains, so that the average domain size grows as the square root of a reduced time t'. Thus, in this model, the slow relaxation of q_0 would follow a behavior $q_0(t) \sim q_{0f} - bt^{-1/2}$, where b is an unknown constant that depends upon the rate of coarsening and the effect of defects. In fact, this algebraic relaxation can well fit the observed behavior as shown by the solid line in Fig. 7.

Finally, we have also seen that the observed anisotropies in peak shapes can largely be understood by considering the differing effects of conservative and nonconservative APB's

on the x-ray scattering pattern. This has been taken into account by a stochastic model of the alloy structure during ordering. While such qualitative understanding is revealing, however, detailed understanding of the complex kinetics observed here will require further advances in theory and/or simulations.

ACKNOWLEDGMENTS

The authors would particularly like to acknowledge the help and encouragement that we received in this work, and other work over many years, from the late Cullie Sparks of Oak Ridge National Laboratory. We also thank Gene Ice and Jiaming Bai of Oak Ridge for their help and advice with the diffuse scattering measurements performed at beamline X14. The authors also would like to thank Didier Regen and Denis Boivin for preparation and characterization of the samples and Oana Malis for help in data collection and analysis. This work was partially supported by NSF Grant No. DMR-9633596. The NSLS is supported by the U.S. DOE Division of Materials Sciences and Division of Chemical Sciences.

[1] F. W. Jones and C. Sykes, J. Inst. Met. **65**, 419 (1939).
[2] C. Michikami, H. Iwasaki, and S. Ogawa, J. Phys. Soc. Jpn. **31**, 956 (1971).
[3] M. Guymont and D. Gratias, Phys. Status Solidi A **36**, 329 (1976).
[4] O. Terasaki and D. Watanabe, Jpn. J. Appl. Phys. **20**, L381 (1981).
[5] D. Broddin, G. Van Tendeloo, J. Van Landuyt, S. Amelinckx, R. Portier, M. Guymont, and A. Loiseau, Philos. Mag. A **54**, 395 (1986).
[6] B. E. Warren, *X-ray Diffraction* (Dover, New York, 1990).
[7] P. R. Subramanian and D. E. Laughlin, Bull. Alloy Phase Diagrams, 1998.
[8] H. Sato and R. S. Toth, Phys. Rev. **124**, 1833 (1961).
[9] S. C. Moss, Phys. Rev. Lett. **22**, 1108 (1969).
[10] B. L. Gyorffy and G. M. Stocks, Phys. Rev. Lett. **50**, 374 (1983).
[11] J. Staunton, D. Johnson, and F. Pinski, Phys. Rev. B **50**, 1450 (1994).
[12] G. Ceder, P. Huang, S. Menon, D. de Fontaine, D. M. Nicholson, G. M. Stocks, and B. L. Gyorffy, Mater. Res. Soc. Symp. Proc. **186**, 65 (1991).
[13] D. de Fontaine and J. Kulik, Acta Metall. **33**, 145 (1985).
[14] *ASM Handbook* (ASM International, Metals Park, OH, 1992), Vol. 3.
[15] X. Wang, K. F. Ludwig, Jr., O. Malis, J. Mainville, X. Flament, and R. Caudron, Phys. Rev. B **63**, 092201 (2001).
[16] A. Finel (unpublished).
[17] X. Flament, Dissertation, Université de Cergy-Pontoise, 2000.
[18] H. E. Cook, D. de Fontaine, and J. E. Hilliard, Acta Metall. **17**, 765 (1969).
[19] T. Ohta, D. Jasnow, and K. Kawasaki, Phys. Rev. Lett. **49**, 1223 (1982).
[20] P. Hohenberg and B. Halperin, Rev. Mod. Phys. **49**, 435 (1977).
[21] S. M. Allen and J. W. Cahn, Acta Metall. **27**, 1085 (1979).
[22] I. J. Jeon, J. H. Hong, and Y. P. Lee, J. Appl. Phys. **75**, 7825 (1994).
[23] T. Ala-Nissila, J. D. Gunton, and K. Kaski, Phys. Rev. B **33**, 7583 (1986).
[24] T. Ala-Nissila, J. D. Gunton, and K. Kaski, Phys. Rev. B **37**, 179 (1988).
[25] S. Hendricks and E. Teller, J. Chem. Phys. **10**, 147 (1942).
[26] Such an interface defect controlled spacing has been suggested in a somewhat different context for Cu_3Au alloys by M. Sutton and A. Fluerasu; A. Fluerasu, Ph. D. thesis, McGill University, 2003.